

TNF- α blockade decreases oxidative stress in the paraventricular nucleus and attenuates sympathoexcitation in heart failure rats

Anuradha Guggilam, Masudul Haque, Edmund Kenneth Kerut, Elizabeth McIlwain, Pamela Lucchesi, Inder Seghal and Joseph Francis

Am J Physiol Heart Circ Physiol 293:H599-H609, 2007. First published 6 April 2007;
doi: 10.1152/ajpheart.00286.2007

You might find this additional info useful...

This article cites 41 articles, 25 of which you can access for free at:
<http://ajpheart.physiology.org/content/293/1/H599.full#ref-list-1>

This article has been cited by 16 other HighWire-hosted articles:
<http://ajpheart.physiology.org/content/293/1/H599#cited-by>

Updated information and services including high resolution figures, can be found at:
<http://ajpheart.physiology.org/content/293/1/H599.full>

Additional material and information about *American Journal of Physiology - Heart and Circulatory Physiology* can be found at:
<http://www.the-aps.org/publications/ajpheart>

This information is current as of February 6, 2013.

American Journal of Physiology - Heart and Circulatory Physiology publishes original investigations on the physiology of the heart, blood vessels, and lymphatics, including experimental and theoretical studies of cardiovascular function at all levels of organization ranging from the intact animal to the cellular, subcellular, and molecular levels. It is published 12 times a year (monthly) by the American Physiological Society, 9650 Rockville Pike, Bethesda MD 20814-3991. Copyright © 2007 by the American Physiological Society. ISSN: 0363-6135, ESSN: 1522-1539. Visit our website at <http://www.the-aps.org/>.

TNF- α blockade decreases oxidative stress in the paraventricular nucleus and attenuates sympathoexcitation in heart failure rats

Anuradha Guggilam,¹ Masudul Haque,¹ Edmund Kenneth Kerut,²
Elizabeth McIlwain,² Pamela Lucchesi,² Inder Seghal,¹ and Joseph Francis^{1,2}

¹Comparative Biomedical Sciences, School of Veterinary Medicine, Louisiana State University, Baton Rouge; and ²Department of Pharmacology, Louisiana State University Health Sciences Center, New Orleans, Louisiana

Submitted 7 March 2007; accepted in final form 30 March 2007

Guggilam A, Haque M, Kerut EK, McIlwain E, Lucchesi P, Seghal I, Francis J. TNF- α blockade decreases oxidative stress in the paraventricular nucleus and attenuates sympathoexcitation in heart failure rats. *Am J Physiol Heart Circ Physiol* 293: H599–H609, 2007. First published April 6, 2007; doi:10.1152/ajpheart.00286.2007.—Oxidative stress plays an important role in the pathophysiology of cardiovascular disease. Recent evidence suggests that cytokines induce oxidative stress and contribute to cardiac dysfunction. In this study, we investigated whether increased circulating and tissue levels of tumor necrosis factor (TNF)- α in congestive heart failure (CHF) modulate the expression of NAD(P)H oxidase subunits, Nox2 and its isoforms, in the paraventricular nucleus (PVN) of the hypothalamus and contribute to exaggerated sympathetic drive in CHF. Heart failure was induced in Sprague-Dawley rats by coronary artery ligation and was confirmed using echocardiography. Pentoxifylline (PTX) was used to block the production of cytokines for a period of 5 wk. CHF induced a significant increase in the production of reactive oxygen species (ROS) in the left ventricle (LV) and in the PVN. The mRNA and protein expression of TNF- α , Nox1, Nox2, and Nox4 was significantly increased in the LV and PVN of CHF rats. CHF also decreased ejection fraction, increased Tei index, and increased circulating catecholamines (epinephrine and norepinephrine) and renal sympathetic activity (RSNA). In contrast, treatment with PTX in CHF rats completely blocked oxidative stress and decreased the production of TNF- α and Nox2 isoforms both in the LV and PVN. PTX treatment also decreased catecholamines and RSNA and prevented further decrease in cardiac function. In summary, TNF- α blockade attenuates ROS and sympathoexcitation in CHF. This study unveils new mechanisms by which cytokines play a role in the pathogenesis of CHF, thus underscoring the importance of targeting cytokines in heart failure.

congestive heart failure; nervous system; cytokines; reactive oxygen species; tumor necrosis factor- α

CONGESTIVE HEART FAILURE (CHF) is characterized by a generalized state of neurohumoral excitation that contributes to progressive deterioration of cardiac function, resulting in the premature death of patients. In the past, most of the treatments were aimed at blocking this exaggerated neurohumoral excitation by using β -adrenergic receptor antagonists, angiotensin converting enzyme inhibitors, and angiotensin receptor blockers in heart failure (HF) patients. These treatments have considerably reduced mortality and morbidity; however, the clinical course of CHF is still progressive, so there is a need for innovative approaches to therapy.

Address for reprint requests and other correspondence: J. Francis, Louisiana State Univ., School of Veterinary Medicine, Comparative Biomedical Sciences Dept., 1909 Skip Bertman Dr., Baton Rouge, LA 70803 (e-mail: jfrancis@lsu.edu).

In addition to neurohormones, the activation of proinflammatory cytokines such as tumor necrosis factor (TNF)- α is known to play a role in the pathogenesis of cardiovascular disease. These cytokines are increased with the severity of heart disease and are of prognostic significance. Despite the abundant evidence that TNF- α contributes significantly to cardiac dysfunction in heart failure in animal models, the results of two large clinical trials using etanercept, a truncated, soluble TNF receptor antagonist (RENAISSANCE), and infliximab (RECOVER), a TNF- α blocking antibody, were largely negative (21). However, pentoxifylline (PTX), a phosphodiesterase inhibitor that also blocks cytokine expression, has been found to be promising in small clinical trials (33). In addition to elevating intracellular cAMP, PTX increases the production of prostacyclins and vasodilatory eicosanoids (25, 28) and depresses the production of TNF- α (35).

The concept of targeting brain production of neurohormones is relatively new and understudied. Recent evidence from our laboratory suggests that cytokines are not only increased in the circulation and left ventricular (LV) tissues but also in the hypothalamus of CHF rats (6). We also showed that cardiac sympathetic afferents contribute to hypothalamic production of cytokines and that the vagal efferents regulate the peripheral production of cytokines, thus suggesting a nervous system link in the activation of cytokines in CHF (10). In the brain, the paraventricular nucleus (PVN) of the hypothalamus is an important center regulating cardiovascular and fluid homeostasis. Electrophysiological studies show that stimulation of PVN results in increased sympathetic activity (17). PVN neuronal activity is increased in HF rats. Injection of TNF- α in the PVN or rostral ventrolateral medulla (RVLM) increased sympathetic activity, suggesting a direct role of TNF- α in sympathetic activity (42). Nevertheless, the mechanisms by which cytokines contribute to the sympathoexcitation in heart failure are not known.

Oxidative stress plays an important role in the progression of CHF. Both in vitro and in vivo studies have associated TNF- α as an important contributor to oxidative stress, either directly or indirectly, by decreasing coronary or systemic perfusion resulting in cardiac dysfunction. Furthermore, TNF- α modulates the activity and expression of NAD(P)H oxidases (Noxs), a potential source of reactive oxygen species (ROS) in cardiovascular disease. NAD(P)H oxidase is a multisubunit enzyme complex that consists of two membrane subunits, p22phox and Nox2, and four cytoplasmic subunits, p40phox, p47phox,

The costs of publication of this article were defrayed in part by the payment of page charges. The article must therefore be hereby marked "advertisement" in accordance with 18 U.S.C. Section 1734 solely to indicate this fact.

p67phox, and Rac1. The catalytic subunit of NAD(P)H oxidases is Nox2, and few isoforms of Nox2, such as Nox1 and Nox4, are found in cardiomyocytes and neurons. The role of TNF- α in eliciting NAD(P)H oxidase subunit expression in CHF is relatively unknown.

Taken together, it is evident that TNF- α contributes significantly to oxidative stress and sympathoexcitation in the pathogenesis of CHF. To understand the mechanistic link between CHF-induced production of cytokines, and neurohumoral excitation, we hypothesized that increased levels of TNF- α in CHF may modulate the expression of Nox2 or its isoforms in the PVN and contribute to the exaggerated sympathetic activity. In this study, we used PTX to block the production of cytokines both at the center and the periphery, since it is the only available drug known to cross the blood-brain barrier (BBB).

MATERIALS AND METHODS

Animals. Adult male Sprague-Dawley rats weighing 350–375 g were used for this study. They were housed in temperature ($23 \pm 2^\circ\text{C}$), and light-controlled (lights on between 7:00 A.M. and 7:00 P.M.) animal quarters and were provided with water and rat chow ad libitum. The experimental procedures were approved by the Louisiana State University Institutional Animal Care and Use Committee.

Experiment protocol. Rats underwent coronary artery ligation (CAL) to induce HF under ketamine + xylazine anesthesia (90 and 10 mg/kg ip) or sham operation (Sham), as described previously (9). Induction of HF was confirmed by transthoracic echocardiography 24 h after recovery from surgery, and the rats were assigned to different treatment groups. Thereafter, HF or Sham rats were chronically injected with PTX (30 mg/kg daily ip; in 10% ethanol) or vehicle (10% ethanol alone) for 5 wk. A second echocardiogram was obtained at the end of the treatment protocol, and the rats were killed under isoflurane anesthesia; plasma and other tissues were collected for further analysis.

Echocardiographic assessment of LV function. A first echocardiography was performed 24 h after CAL followed by a second echo at the end of 5 wk of study, as described previously (8). In brief, transthoracic echocardiography was performed while the animals were under ketamine anesthesia, using a Toshiba Aplio SSH770 (Toshiba Medical, Tustin, CA) fitted with a PST 65A sector scanner (8-MHz probe) that generates two-dimensional images at a frame rate ranging from 300 to 500 frames/s. LV end diastolic volume (LVEDV) and ejection fraction (EF) were computed using the area length method. The portion of the LV that displays akinesis was electronically planimeted and expressed as a percent of the total LV silhouette to estimate the size of the ischemic zone (%IZ). Only rats with large infarct (%IZ $\geq 45\%$) were used for the study. LV fractional shortening (FS%) was calculated using the following equation: $\text{FS}\% = [(\text{LVDD} - \text{LVESD})/\text{LVEDD}] \times 100$, where LVDD is LV internal diameter at end diastole, LVESD is LV end-systolic diameter, and LVEDD is LV end-diastolic diameter. Tei index was determined from Doppler recordings of LV inflow and outflow as described previously (3). From mitral inflow, isovolumetric relaxation time and isovolu-

metric contraction time were measured. Ejection time was measured from the LV outflow velocity curve recorded from the long-axis view. The Tei index was calculated using the equation, $\text{Tei index} = (\text{isovolumetric relaxation time} + \text{isovolumetric contraction time})/\text{ventricular ejection time}$.

Detection of ROS in the heart and brain. ROS were detected using dihydroethidium (DHE) staining. DHE is a fluorogenic probe that in the presence of ROS is converted to ethidium bromide that intercalates with nuclear DNA, resulting in a punctuate appearance. The rats received an intracardiac injection of DHE at a dose of 80 $\mu\text{g}/\text{kg}$ body wt. Hearts and brains were harvested, placed in a freezing mold with Tissue-Tek optimum cutting temperature compound (Sakura Finetek, Torrance, CA), snap-frozen with liquid nitrogen, sectioned on a cryostat, and placed on slides. Cryosections (12 μm) were immediately viewed and imaged under epifluorescence with a Zeiss Axiovert 200 microscope using an ethidium bromide-compatible filter set (Chroma Filters no. 41006); images were captured with an Olympus Q Capture 5 camera and Q Capture Pro software.

Extraction of PVN by laser capture microscopy. Laser capture microscopy was conducted in a dehumidified room (humidity $\leq 35\%$) and was kept to <30 min/slide to reduce the loss in recovery of intact RNA. A 7.5- μm laser spot size was used to capture the PVN at a power range of 65–80 mW and pulse duration of 550–750 μs . This combination of parameters allowed efficient retrieval of the entire PVN area and a consistent lifting efficiency of $>80\%$. The number of laser “shots” used for each sample was kept constant at 1,400. These parameters secured a sufficient and near-constant amount of input RNA for comparative real-time RT-PCR analyses and protein for Western blotting. All experiments were performed no less than five times with five different animals.

Measurement of circulating TNF- α . At the end of the 5-wk study, one group of rats was killed by decapitation with guillotine under deep anesthesia by isoflurane, and ~ 4 ml of trunk blood were collected in heparinized tubes. Plasma samples obtained by centrifugation of heparinized blood at 4°C (Beckman-Coulter) at 2,500 revolutions/min for 15 min were used for estimation of circulating TNF- α and catecholamines. Circulating levels of TNF- α were quantified using a commercially available rat TNF- α ELISA kit (Biosource, Camarillo, CA) as described previously (5, 37).

Estimation of circulating catecholamine levels. Plasma norepinephrine and epinephrine were measured using HPLC as described previously (7) with minor modifications in plasma sample preparation. Plasma samples were prepared by adding activated alumina, Tris buffer, EDTA, and internal standard 3,4-dihydrobenzylamine, along with 0.5 ml of rat plasma. The samples were centrifuged, and supernatant was separated, rinsed two times in ultrapure water, and filtered through a Millipore filter (Ultrafree MC UFC30GV00; Millipore). Samples were filtered and injected in an Eicom HTEC-500 system fitted with an HPLC-ECD.

Renal sympathetic nerve activity. One set of rats was subjected to recording of renal sympathetic nerve activity (RSNA). The left kidney was exposed by left retroperitoneal flank incision. The renal sympathetic nerves were identified under a dissecting microscope, isolated free of the surrounding connective tissue, and placed on a pair of platinum recording electrodes. Once an optimal signal-to-noise ratio was achieved, the electrode and the renal nerve were covered with a

Table 1. Sequence of primers used to detect TNF- α , Nox1, Nox2, and Nox4 by realtime RT-PCR

Primer	Sense	Antisense	Genebank ID
TNF- α	3'-GTCGTAGCAAACCAAGC-5'	5'-TGTGGGTGAGGAGCATAG-3'	D00475
Nox1	3'-CCCTGGAACAAGAGATGGAC-5'	5'-AATTGGTCTCCCAAAGGAGGT-3'	NM_053683
Nox2	3'-CGGAATCCTCTCCTTCCT-5'	5'-GCATTACACACCCTCCAC-3'	AF298656
Nox4	3'-TTCTACATGCTGTGCTGCT-5'	5'-AAAACCTCCAGGCAAAGAT-3'	AY027527

TNF- α , tumor necrosis factor- α ; Nox, NAD(P)H oxidase. The primer sequences were designed with Primer 3 (version 0.3.0) software.

Table 2. Echocardiographic findings

	Sham	Sham + PTX	MI (24 h)	CHF (5 wk)	CHF + PTX (5 wk)
<i>n</i>	18	18	48	23	23
HR	415 \pm 12.0	410 \pm 5.00	409 \pm 12.0	418 \pm 6.00	411 \pm 10.0
IVSD, mm	1.52 \pm 0.05	1.55 \pm 0.04	1.22 \pm 0.09	1.14 \pm 0.08*	1.53 \pm 0.10†
IVSS, mm	2.80 \pm 0.09	2.72 \pm 0.08	1.76 \pm 0.12*	1.67 \pm 0.13*	2.00 \pm 0.16*
LVDD, mm	6.41 \pm 0.18	6.33 \pm 0.14	7.75 \pm 0.40	10.91 \pm 0.72*	8.99 \pm 0.17*†
LVDS, mm	3.03 \pm 0.18	3.01 \pm 0.06	5.92 \pm 0.45*	8.12 \pm 0.63*	7.80 \pm 0.86*
PWD, mm	1.67 \pm 0.05	1.74 \pm 0.08	1.17 \pm 0.04*	1.26 \pm 0.12*	1.45 \pm 0.06
PWS, mm	2.66 \pm 0.10	2.70 \pm 0.06	1.87 \pm 0.12*	1.85 \pm 0.15*	2.17 \pm 0.07*
EF, %	83.7 \pm 0.90	84.6 \pm 1.20	34.0 \pm 0.20*	26.0 \pm 1.20*	33.2 \pm 2.40*†
FS, %	52.94 \pm 1.96	51.79 \pm 1.30	24.45 \pm 2.34*	15.42 \pm 1.26*	23.42 \pm 2.41*
IZ, %	0	0	54.9 \pm 1.80	58.9 \pm 2.60	55.8 \pm 3.10
Tei	0.46 \pm 0.02	0.44 \pm 0.02	0.34 \pm 0.03	0.51 \pm 0.04	0.32 \pm 0.03*†
LVEDV, μ l	548 \pm 56	520.3 \pm 48.5	865 \pm 40.2*	1015 \pm 93.6*	868 \pm 103*†

Values are means \pm SE; *n*, no. of rats. HR, heart rate; EF, ejection fraction; FS, fractional shortening; IZ, ischemic zone; LVEDV, left ventricle end-diastolic volume; PTX, pentoxifylline; MI, myocardial infarction; CHF, congestive heart failure; IVSD and IVSS, interventricular septal thickness at end diastole and end systole, respectively; LVDD and LVDS, left ventricular internal diameter at end diastole and end systole, respectively; PWD and PWS, posterior wall thickness at end diastole and end systole, respectively. *P* < 0.05 compared with the sham group (*) and 24-h MI group (†).

dentistry impression material (Coltene President). The signal was amplified with a Grass P511 band-pass amplifier with low-frequency cutoff set at 30 Hz and high-frequency cutoff at 3 kHz. The amplified and filtered signal was channeled to an audio amplifier-loudspeaker (Grass model AM 8 audio monitor) for auditory evaluation and to a rectifying voltage integrator for quantification (Grass model 7P10). The integrated voltage signals were acquired by a commercially available data acquisition system (Acknowledge for Windows; Biopack, Santa Barbara, CA). Minimum and maximum RSNA was detected using an intravenous bolus administration of phenylephrine (20 g/kg) and sodium nitroprusside (SNP; 100 g/kg), respectively. At the end of the experiment, the background noise, defined as the signal recorded postmortem, was subtracted from actual RSNA recorded and subsequently expressed as percent of maximum (in response to SNP).

RNA isolation and real-time RT-PCR. Total RNA was extracted from the LV and microdissected PVN using Tri-Zol reagent (Invitrogen) and reverse transcribed using oligo(dT) and RT. Expression

levels of Nox1, Nox2, Nox4, and TNF- α , mRNA was determined using specific rat primers shown in Table 1. Glyceraldehyde-3-phosphate dehydrogenase (GAPDH) was used as housekeeping gene. Real-time RT-PCR was performed in 384-well PCR plates using Bio-Rad PCR Master Mix (the iTaq SYBR Green Supermix with ROX) and the ABI Prism 7900 sequence detection system (Applied Biosystems). The PCR cycling conditions were as follows: 50°C for 2 min, 95°C for 10 min, followed by 40 cycles (15 s at 95°C, 1 min at 60°C). A dissociation step (15 s at 95°C, 15 s at 60°C, and 15 s at 95°C) was added to check the melting temperature of the specific PCR product.

Western blot analysis of Nox subunits. Protein was extracted from LV samples and laser-captured PVN samples in ice-cold buffer (10 mM Tris·HCl, pH 7.4, 1 mM EDTA, 1% Nonidet P-40, 0.1% sodium deoxycholate, and 0.1% SDS) containing a protease inhibitor cocktail (Roche). The protein content in the supernatant was determined using a detergent-compatible protein assay (Bio-Rad). Protein samples (25

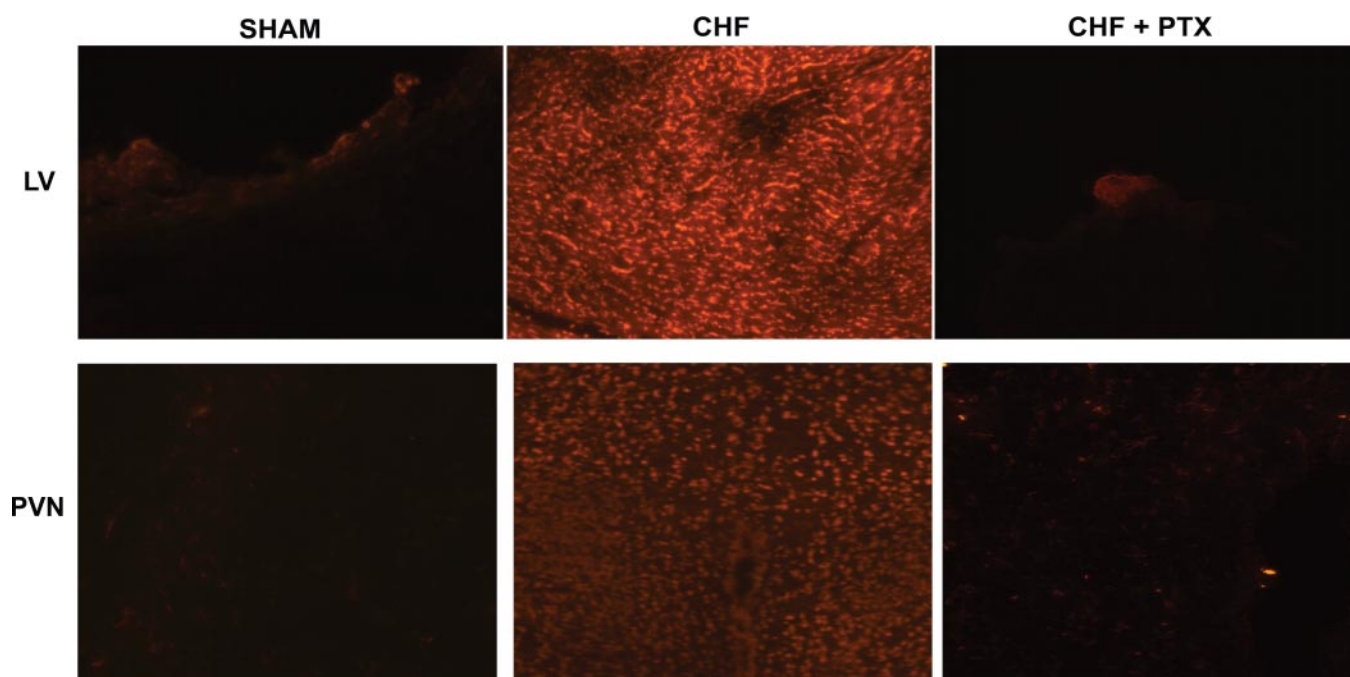


Fig. 1. Detection of reactive oxygen species (ROS) by dihydroethidium (DHE) staining. Under identical imaging conditions, production of superoxide is elevated significantly in the heart (*top*) and brain (*bottom*) sections compared with Sham and pentoxifylline (PTX)-treated rats.

μ g) were resolved in a 10% SDS-polyacrylamide gel along with a molecular weight marker and then transferred to a polyvinylidene difluoride membrane. The membranes were blocked at room temperature for 1 h in 1% casein in PBS-Tween. Blots were then incubated overnight at 4°C with the following primary antibodies: Nox1 (1:1,000 dilution) and Nox2 (1:1,000 dilution) (Santa Cruz Biotechnology). GAPDH (1:1,000 dilution) was used as an internal control. Bound primary antibodies were detected with a horseradish peroxidase-labeled secondary antibody (1:20,000; 1 h) and enhanced chemiluminescence (Amersham). The band intensities were quantified using Kodak ID 3.6 imaging systems and normalized with GAPDH levels.

Localization of TNF- α and Nox subunits by immunohistochemistry. Brain and heart tissues were fixed in 4% paraformaldehyde, cut into 8- μ m-thick sections, and then pretreated with 0.3% hydrogen peroxide and 0.1% sodium azide in PBS for 10 min to inhibit endogenous peroxidase activity. These sections were washed two times in PBS and incubated in blocking medium (1% BSA and 10% normal goat serum in PBS) for 10 min. The sections were then treated with respective primary antibodies Nox1 (1:100 dilution), Nox2 (1:100 dilution), Nox4 (1:100 dilution), and TNF- α (1:100 dilution) (Santa Cruz Biotechnology) and incubated overnight at 4°C. The sections were again washed two times in PBS and incubated with secondary antibody, a peroxidase-conjugated IgG antibody, for 30 min. Bound

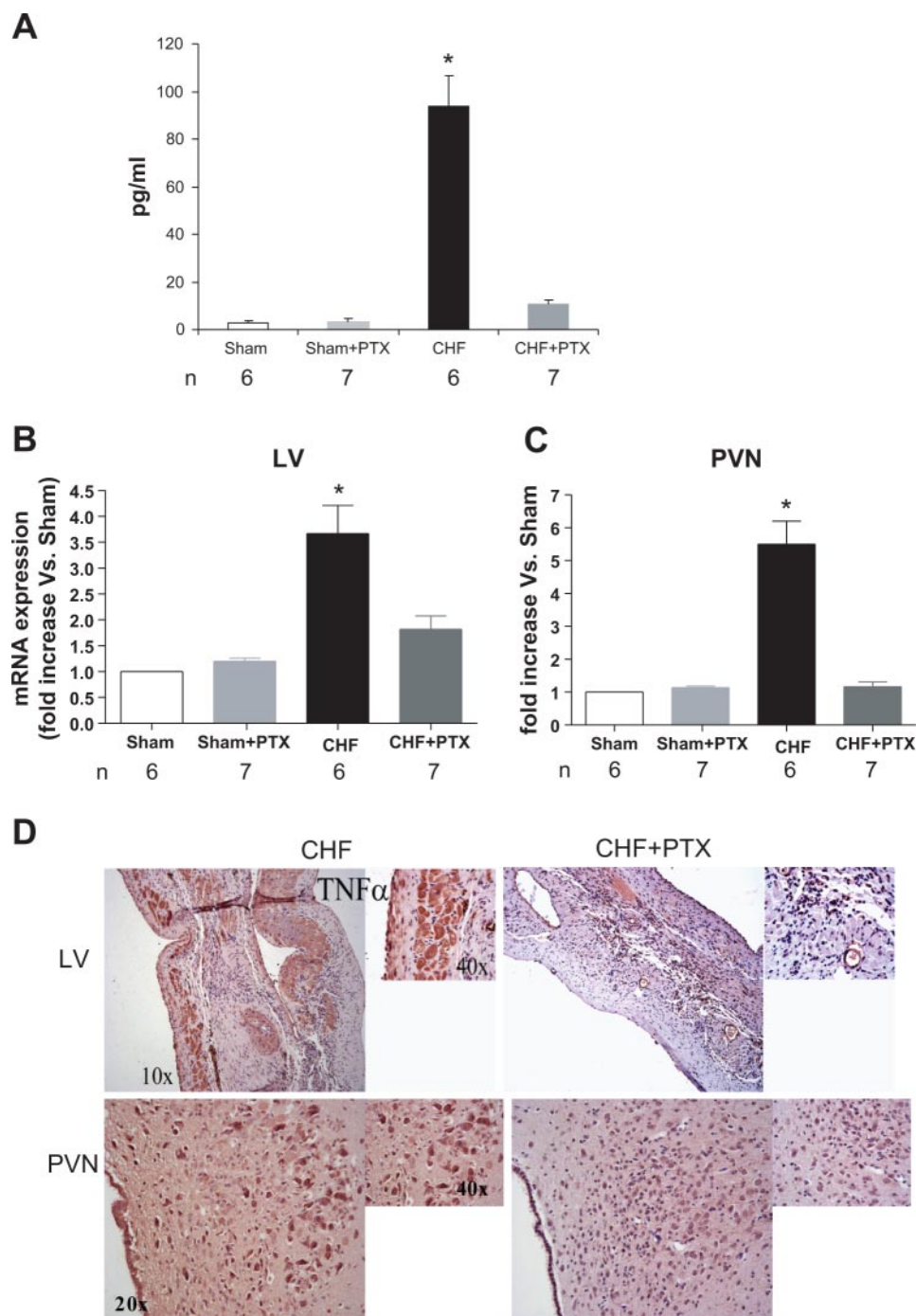


Fig. 2. Tumor necrosis factor (TNF)- α levels. *A*: PTX inhibited congestive heart failure (CHF)-induced production of circulating TNF- α ($*P < 0.05$). *B* and *C*: CHF-induced mRNA expression of TNF- α inhibited by PTX in the left ventricle (LV; *B*) and the paraventricular nucleus (PVN; *C*). *D*: immunohistochemistry photomicrographs of TNF- α in the LV and PVN.

antibodies were detected with streptavidin-peroxidase complex using 0.2 mg/ml 3,3'-diaminobenzidine tetrahydrochloride in PBS containing 0.003% hydrogen peroxide. Negative control sections were incubated with secondary antibody alone.

Statistical analysis of data. All results are expressed as means \pm SE. For statistical analysis of the data, one-way ANOVA followed by Bonferroni's post hoc test was performed using GraphPad Prism version 4.00 for Windows (GraphPad Software, San Diego, CA) to determine differences among groups. A *P* value <0.05 was considered statistically significant.

RESULTS

Effect of PTX treatment on survival of CHF rats. A total of 101 rats were subjected to CAL or Sham surgery and subsequently assigned to three sets of animals, one set for immunohistochemistry, the second for mRNA, and the third for Western blot analysis. The average survival within 24 h of surgery was 80% in the rats undergoing CAL and 100% in the Sham group. Over the 5-wk study, two of the CHF rats and two of the CHF + PTX rats died before the designated time point, whereas none of the Sham animals died during the investigation. Thus, over the course of the 5 wk, PTX treatment had no apparent influence on the survival (Table 2).

Effect of PTX on ROS production in HF. ROS production in the heart and brain was assessed by DHE fluorescence (Fig. 1). As indicated by the punctate staining of the nuclei, CHF induced an increase in ROS production in the heart and brain tissues. In contrast, PTX inhibited CHF-induced ROS production.

Effect of PTX on LV function. Table 2 shows LV function in rats as measured by echocardiography. Compared with Sham animals, CHF rats had reduced EF, increased LVEDV, and increased volume-to-mass ratio. There was no significant difference in the heart rate between the two CHF groups. The average %IZ in both CHF groups was $>56\%$, with a range of 50–58% before and after the treatments. At the end of the 5 wk, Tei index was increased by 59.38% and EF further declined by 21.21% in the CHF group. In contrast, treatment with PTX in the CHF group prevented further decline in EF and decreased Tei index.

Effect of PTX on cytokine production in HF. To determine the effect of PTX treatment on CHF-induced production of TNF- α in the heart and PVN, we determined mRNA transcript levels by real-time RT-PCR in the LV tissue and in the PVN isolated using laser capture microdissection. Circulating levels

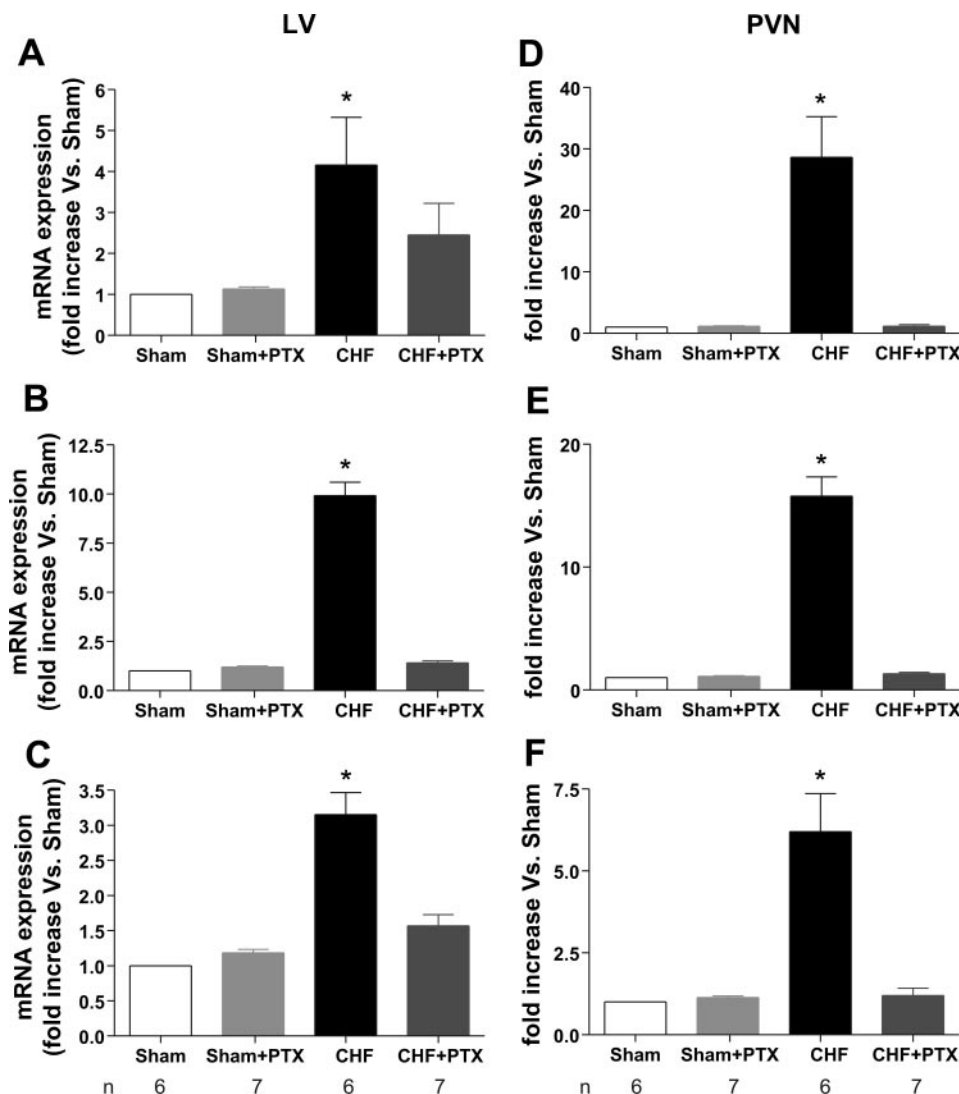


Fig. 3. Effect of PTX treatment on mRNA levels of NAD(P)H oxidase subunits [Nox1 (A), Nox2 (B), and Nox4 (C)] in the LV and PVN [Nox1 (D), Nox2 (E), and Nox4 (F)] of experimental rats. Levels of Nox1, Nox2, and Nox4 were elevated in the LV and PVN of CHF rats compared with the Sham and PTX-treated rats. **P* < 0.05 .

of TNF- α were also measured by ELISA to estimate the anticytokine effects of PTX. As shown in Fig. 2A, the elevated levels of circulating TNF- α found in CHF rats were restored to near normal levels with PTX treatment. The LV of CHF rats showed increased levels of TNF- α (~ 3.7 -fold increase) when compared with those of PTX-treated rats (~ 1.7 -fold increase), although the levels did not exactly reach the levels of Sham rats (Fig. 2, B and C).

To further ascertain the anticytokine effects of PTX in CHF rats, the protein levels of TNF- α were assessed in the LV and PVN by immunohistochemistry. Immunohistochemistry revealed that elevated levels of TNF- α in CHF were significantly attenuated by treatment with PTX (Fig. 2D). These results show that the TNF- α expression is significantly inhibited by PTX both in the LV and the PVN of CHF rats.

Modulation of expression of Nox1, Nox2, and Nox4 in HF. The mRNA expression of the NAD(P)H oxidase subunits Nox2 and its isoforms (Nox1 and Nox4) was assessed by real-time RT-PCR. CHF induced an ~ 6 -, 10 -, and 4 -fold increase in Nox1, Nox2, and Nox4 in the LV (Fig. 3, A–C), respectively. A similar increase was also seen in the PVN of CHF rats (~ 28 -, 15 -, and 6 -fold increase, respectively) for Nox1, Nox2, and Nox4 compared with the Sham group (Fig. 3,

D–F). PTX treatment in the CHF group significantly reduced the expression of these subunits in both the LV and PVN.

Protein expression for Nox1, Nox2, and Nox4 was measured in the LV and PVN by Western blot analyses. Unfortunately, we did not get a good signal on the Western blot with the commercially available Nox4 antibody. As shown in Figs. 4A and 5A, CHF rats treated with PTX exhibited a decrease in the protein expression of Nox1 and Nox2 in the LV and PVN (Figs. 4B and 5B).

Immunohistochemistry also revealed an increased expression of Nox1, Nox2, and Nox4 in the LV of CHF rats compared with Sham and those treated with PTX (Figs. 4C, 5C, and 6, respectively). In the PVN, Nox1 was predominantly detected in the magnocellular neurons of CHF rats (Fig. 4C). Nox2 and Nox4 expression was increased both in the magnocellular and parvocellular neurons of the PVN of CHF rats. Treatment with PTX reversed all these changes in the PVN of CHF rats (Figs. 5C and 6).

Effect of blocking cytokines on sympathetic activity. Plasma epinephrine and norepinephrine levels were significantly increased (995.5 ± 89 and 576 ± 56 pg/ml, respectively; $P < 0.05$) in the CHF rats. After inhibition of cytokines with PTX, these catecholamine levels were decreased significantly ($347 \pm$

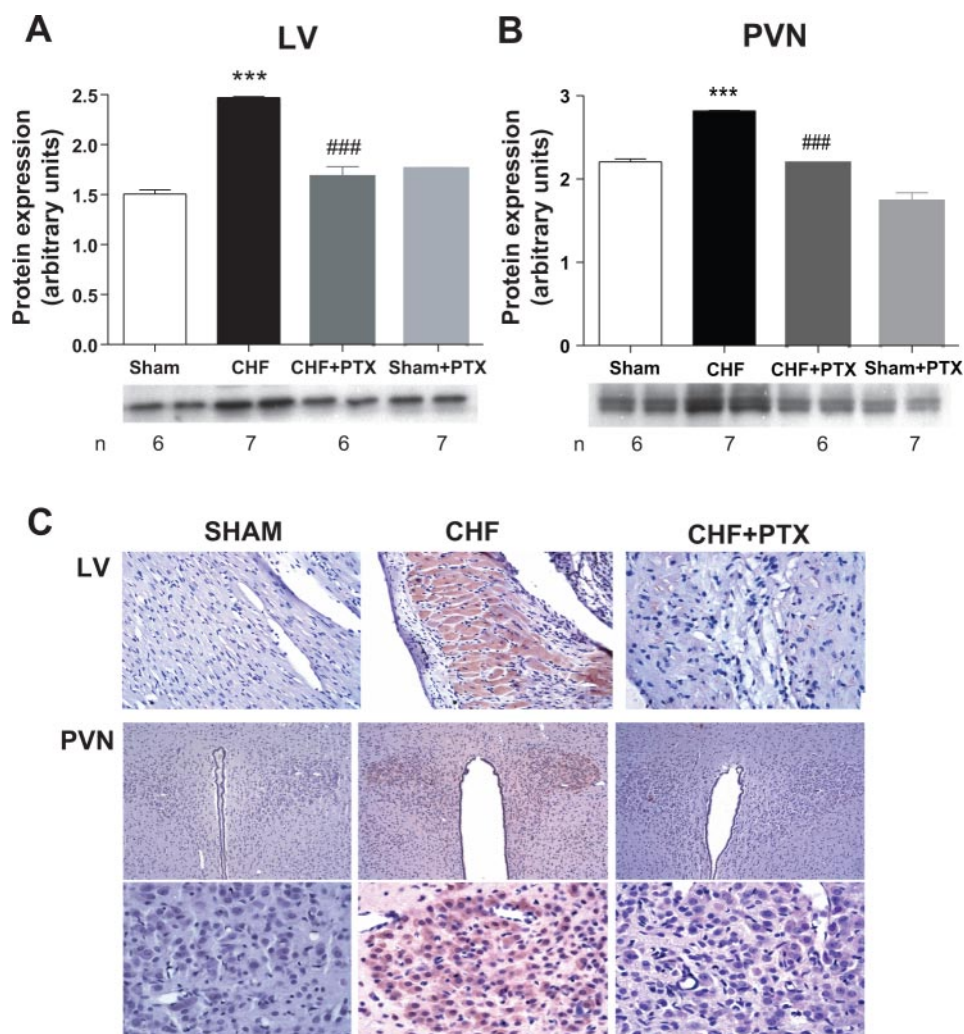


Fig. 4. Effect of PTX treatment on protein expression of Nox1 subunit. Representative Western blot and densitometric analysis of Nox1 in the LV (A) and PVN (B). *** $P < 0.001$ vs. Sham; ### $P < 0.001$ vs. CHF. C: immunohistochemical localization of Nox1 in the LV and PVN of CHF rats. Degree of Nox1 staining was notably increased in the magnocellular neurons but not in the parvocellular neurons of the PVN compared with the Sham and PTX-treated rats with myocardial infarction (MI). Images shown represent similar results observed in preparations from 4 to 6 rats.

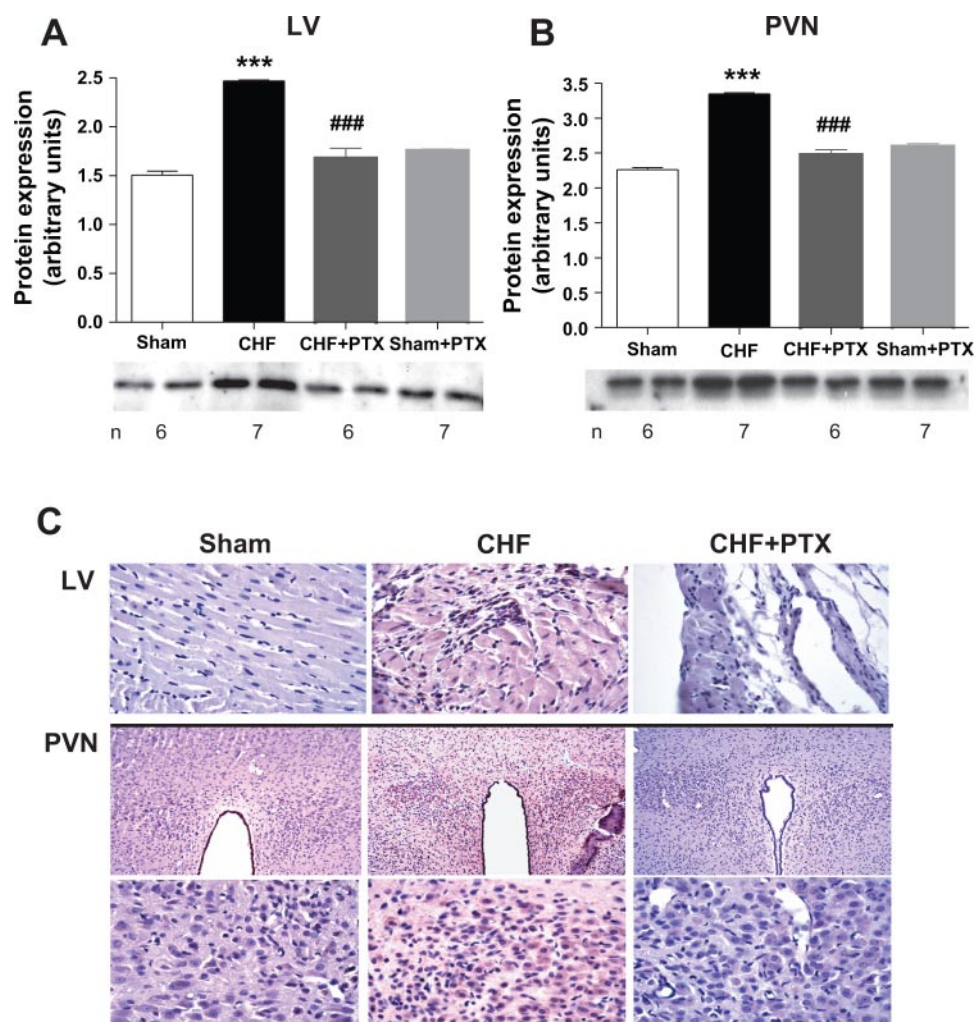


Fig. 5. Nox2 protein expression. Representative blot and densitometric analysis of LV (A) and PVN (B). *** $P < 0.001$ vs. Sham; ### $P < 0.001$ vs. CHF. C: photomicrographs showing expression of Nox2 in the LV and PVN of CHF rats. PTX attenuated Nox2 subunit expression both in the LV and PVN of CHF rats. The sections shown are representative of results from 3 different experiments. Magnification is $\times 100$ in top and $\times 400$ in bottom.

42 and 192.9 ± 29 pg/ml, respectively; $P < 0.05$). These levels showed a significant difference when compared with those of Sham rats (225 ± 30 and 193 ± 40 pg/ml, respectively; $P < 0.05$; Fig. 7A).

Figure 7B shows a raw tracing from a vehicle-treated CHF rat and PTX-treated CHF rat. Figure 7C shows RSNA as a percent of maximum response to the hypotension induced by intravenous injection of SNP. RSNA response to hypotension was maximum in CHF rats treated with vehicle when compared with that of PTX-treated CHF rats. There was no difference in the RSNA activity in vehicle- and PTX-treated Sham rats in response to hypotension.

DISCUSSION

The major findings of this study are as follows: 1) the expression of the NAD(P)H oxidase subunits (Nox1, Nox2, and Nox4) was elevated in the LV and the PVN of CHF rats; 2) administration of PTX, a blocker of proinflammatory cytokine production, normalized the enhanced NAD(P)H oxidase subunit and TNF- α expression, both in the PVN and the LV; and 3) PTX also decreased the circulating catecholamine levels and RSNA, indicators of sympathetic activity, in CHF rats. These findings suggest that the cytokines play a role in induc-

ing oxidative stress in the PVN, thereby contributing to the increased sympathetic activity in CHF rats.

PTX and LV function. Cytokines are produced locally in the myocardium in response to stimuli such as hemodynamic pressure overload and myocardial ischemia or infarction (2, 38). Several clinical studies have shown that PTX decreases proinflammatory cytokine production and improves LV function in CHF patients (1, 29–32, 34). In this study also, we show that treatment with PTX in CHF rats resulted in a significant improvement in LVEF and prevented an increase in the Tei index, an indicator of systolic dysfunction. The Tei index is a combination of contraction and relaxation time intervals constituting an overall index of LV function as assessed by Doppler echocardiography. The Tei index has been shown to have prognostic importance in dilated (3) and restrictive cardiomyopathies (13) and also in acute myocardial infarction (24). The Tei index has a narrow range in normal subjects and seems to progressively increase with deterioration of LV function (3). TNF- α exerts a negative inotropic effect on the contractility of the ischemic heart in hamsters, dogs, and humans (4) by interfering with calcium homeostasis and thus interfering with contraction-excitation coupling (22). PTX has been demonstrated to exert protective effects on ischemic

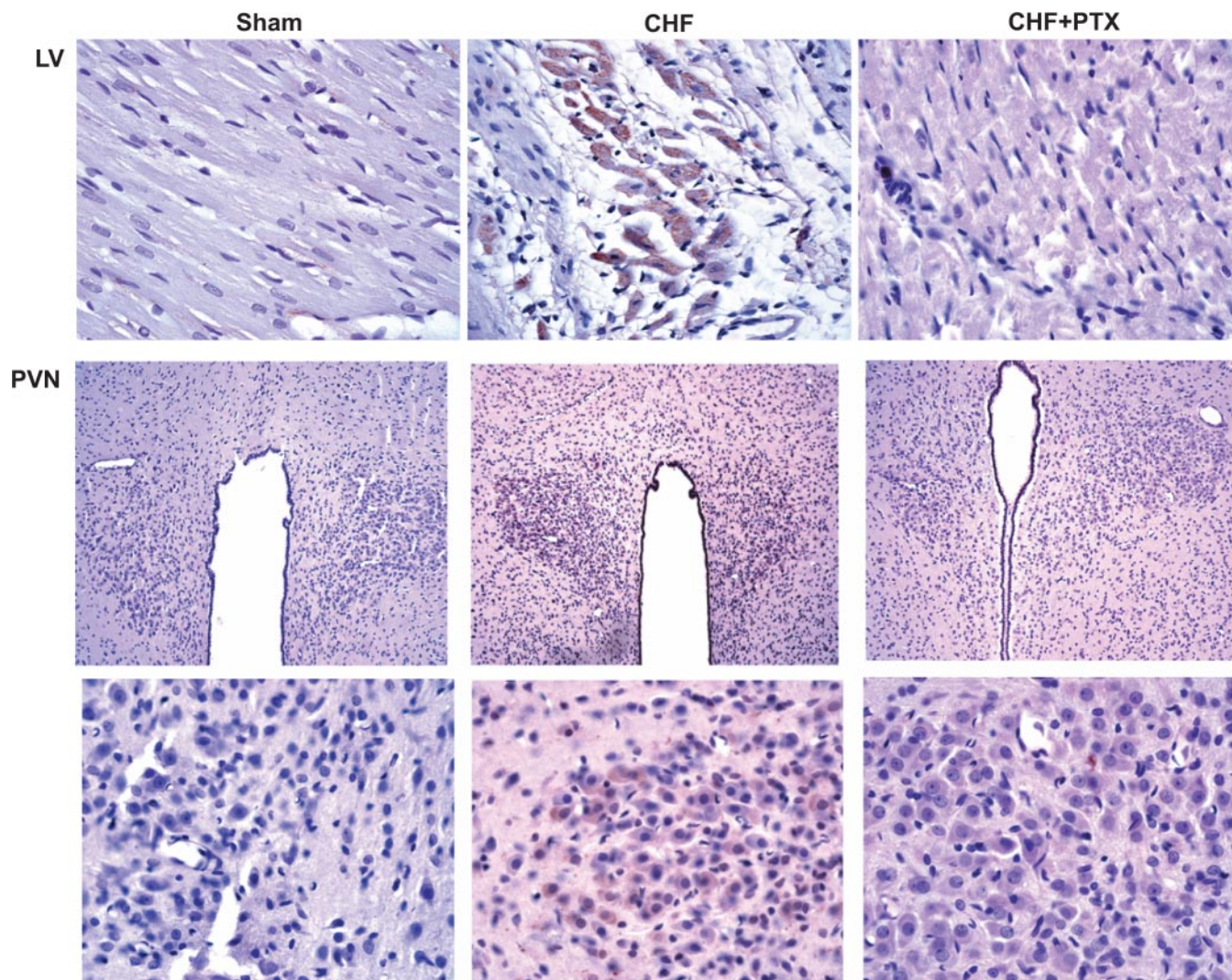


Fig. 6. Photomicrographs showing expression of Nox4 in the LV (top) and PVN (bottom). CHF increased the expression of Nox4 both in the LV and PVN of heart failure rats, whereas PTX treatment attenuated this increased expression.

myocardium by reducing TNF- α production (40). In the present study, we saw a deterioration of LV function in the vehicle-treated CHF rats as indicated by decreased EF and increased Tei index. We also observed an increase in LVDD and LVEDV, which indicates a decrease in LV contractile function. Treatment with PTX improved LV contractile function in our study, which could be because of a combined reduction in cytokines and oxidative stress. This is supported by our observation that PTX treatment decreased ROS production. It has been shown that the surviving myocytes in the infarcted region are potential sources of cytokines, which may contribute to the progression of CHF (15). This study further shows that PTX, by virtue of its anti-cytokine activity, exerts its role in improving the systolic function in CHF, which is comparable to other studies (12, 15, 29).

Cytokines and CNS in CHF. When the stress-activated cytokines in the myocardium exceed the limit to be utilized by the local cellular receptors in autocrine/paracrine functions, they become bloodborne and enter the systemic circulation, causing some of the adverse effects associated with cytokines. One critical function of blood-borne cytokines is to stimulate

self-production via a feed-forward mechanism. These blood-borne cytokines are large molecules and do not readily cross the BBB. However, they can enter the brain through a saturable transport mechanism or a passive transport mechanism via the circumventricular organ, where the BBB is either weak or absent. Our previous studies showed that cardiac sympathetic afferents are a potential mechanism for the induction of hypothalamic cytokines in CHF (10). Thus the circulatory cytokines could induce inflammatory and sympathoexcitatory mediators in the brain that have been shown to be antagonized by a mineralocorticoid receptor blocker (16). The deleterious role of these stress-activated cytokines in the progression of heart disease could be because of the direct toxic effects exerted by these cytokines on heart and circulation.

The PVN of the hypothalamus is one of the five major regions in the brain controlling sympathetic outflow. It regulates sympathetic activity via its inputs from the nucleus tractus solitarius (36) and efferent projections to the RVLM and intermediolateral column of the spinal cord (27). The PVN is composed of two kinds of neurons (36): the larger magnocellular neurons projecting in the pituitary are responsible for

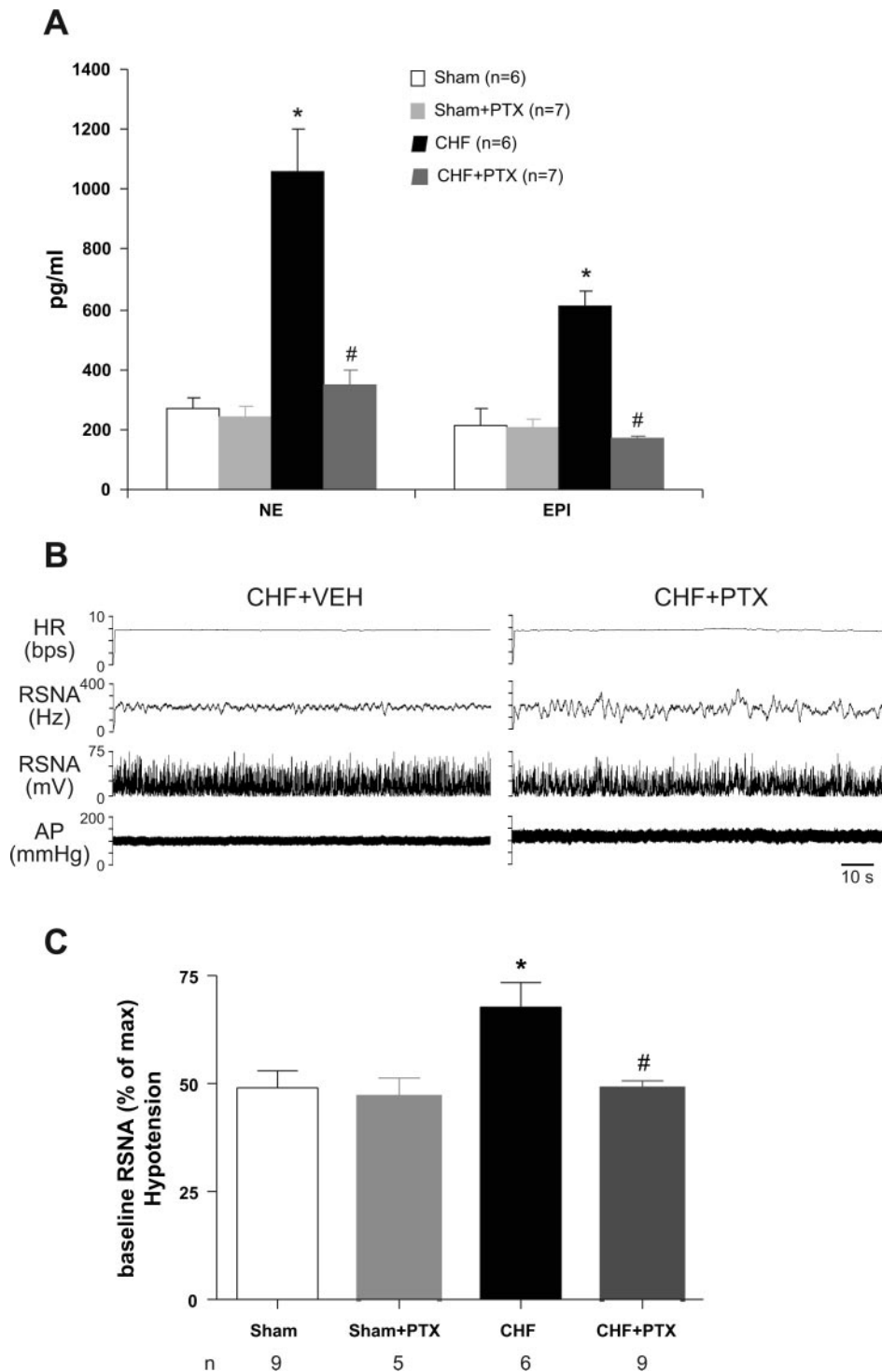


Fig. 7. Sympathetic activity. *A*: circulating norepinephrine (NE) and epinephrine (Epi) levels were significantly higher in CHF rats, whereas they were lower in those treated with PTX. $P < 0.05$ compared with Sham. *B*: and *C*: raw tracing showing renal sympathetic nerve activity (RSNA; *B*) and integrated RSNA (*C*) of CHF rats was higher in the vehicle-treated rats compared with the PTX-treated rats. $*P < 0.05$ vs. Sham; $\#P < 0.05$ vs. CHF.

humoral regulation of fluid balance, whereas the smaller parvocellular neurons projecting to other sites in the CNS are involved in mediating sympathetic activity (26).

It has also been shown that many putative mediators, like prostaglandins, facilitate the transport of cytokines in the brain. These cytokines then stimulate the microglial cells in the brain to produce even more cytokines. We have also shown that injection of PGE₂ increased sympathetic activity in HF rats (42). In this study, we show cardiosympathoexcitatory neurons

of the PVN as yet another potential source of cytokines in CHF. Moreover, the enhanced sympathetic activity in HF rats was decreased in the present study concurrent with the administration of PTX, as evidenced by attenuated circulating catecholamine levels and RSNA. To observe the effects of central administration of PTX on RSNA, we administered PTX (10 μ g/kg body wt) chronically for 5 wk using osmotic minipumps in a group of rats ($n = 8$) through intracerebroventricular cannulation in CHF rats. No significant difference in RSNA or

other parameters was observed in the rats treated with PTX either peripherally or centrally (data not shown). This shows that intraperitoneal administration of PTX exerts both central and peripheral effects. Although the antagonism of TNF- α was not successful in larger clinical trials (possibly because of the fact that the Etanercept could bind to only the circulating and not the membrane-bound tissue TNF- α ; see Ref. 18), a small clinical trial using PTX was successful in improving cardiac outcomes (33). Our results in the present study strongly suggest that using PTX decreases the tissue-bound TNF- α in the PVN and LV.

Oxidative stress and CHF. Apart from cytokines, ROS have also been implicated in the pathogenesis of CHF. The NAD(P)H oxidases are one of the major sources of superoxide in the heart. This multisubunit enzyme complex consists of two membrane subunits, p22phox and Nox2, and four cytoplasmic subunits, p40phox, p47phox, p67phox, and Rac1. Nox2 is the catalytic subunit of NAD(P)H oxidase, and it has other isoforms, namely Nox1 and Nox4, that substitute Nox2 in cardiomyocytes and neurons.

NAD(P)H oxidases activated by ANG II, cytokines (e.g., TNF- α), endothelin-1, and mechanical forces are shown to play an important role in cardiovascular dysfunction (11). Nox1 has been reported to be upregulated in TNF- α -induced oxidative stress in coronary arteries of hyperhomocysteinemic rats (39), whereas Nox4 is upregulated in aortic smooth muscle cells treated with TNF- α (23). Nox2 is demonstrated to be elevated in human CHF (14), and this was also confirmed in cardiomyocytes (19). In this study, we show that Nox2 and its homologues, Nox1 and Nox4, are upregulated in the LV and PVN of CHF rats. These results are also positively correlated to the ROS production, as indicated by the DHE staining (Fig. 1). Inhibition of TNF- α production by PTX has reversed these changes, suggesting a role for cytokines in redox-sensitive signaling in CHF.

PVN and supraoptic nucleus are most strongly implicated in the redox mechanisms in the postmyocardial infarction neurodysregulation (20). In our study, we too show that there is increased ROS in the PVN; more specifically, we show that ROS-producing machinery is increased in the PVN of CHF rats. Among the Noxs shown, Nox1 is predominantly seen in the magnocellular neurons of the PVN. Thus it is possible that Nox1 could play a role in regulating the neurohumoral mechanism contributing to CHF. Interestingly, Nox4 expression is increased both in the magnocellular and parvocellular neurons of the PVN. Nox2 is also increased in the magnocellular and parvocellular neurons of PVN in CHF rats. These findings suggest that expression of different Nox2 homologues in these cell bodies has a significant role in the pathogenesis of CHF and raise the possibility that Nox2 and Nox4 overexpression in the parvocellular neurons contributes significantly to neurohumoral excitation in CHF. Further studies are needed to identify the role of these homologues in sympathoexcitation.

Recent studies showed that microinjection of a NAD(P)H oxidase inhibitor in the PVN reduced the cardiac sympathetic afferent reflexes elevated by central ANG II or the epicardial application of bradykinins (41). Coupled with our findings that a cytokine blocker, PTX, inhibits CHF-induced Nox expression in the PVN and LV, it suggests that oxidant signaling via cytokines in the PVN may be involved in the reduction of catecholamine levels and RSNA in CHF. It is plausible that

one might extrapolate that the effects of PTX observed in the PVN could be because of its other varied effects. However, from the precise anticytokine and antioxidant effects of PTX observed in this study, it is convincing to conclude that decreased cytokines resulted in the reduction of NAD(P)H oxidase subunits in the PVN and, thus, sympathoexcitation in CHF.

In conclusion, our present study clearly demonstrates that the CHF induced an increase in TNF- α in the PVN and in the LV contributes to the increased expression of NAD(P)H oxidase subunits Nox1, Nox2, and Nox4. Treatment with PTX, an inhibitor of cytokine production, attenuated the mRNA and protein expression of these subunits and superoxide production and also decreased circulating levels of catecholamines in CHF rats. Our results suggest that cytokine-induced oxidative stress in the central nervous system and in the periphery contributes to the pathophysiology of CHF. Furthermore, these studies demonstrate that, for the first time, both cytokines and NAD(P)H oxidase in the PVN contribute to increased plasma catecholamine and exaggerated neurohumoral excitation in CHF.

ACKNOWLEDGMENTS

We express our appreciation to Sherry Ring for sectioning the tissue samples and Julie Millard for help with immunohistochemistry.

GRANTS

These studies were supported by National Heart, Lung, and Blood Institute Grant 1RO1 HL-080544-01, American Heart Association scientist development Grant 0330191N, and Louisiana Board of Regents LEQSF (2005-2007) RD-A-06 to J. Francis.

REFERENCES

1. Bahrmann P, Hengst UM, Richartz BM, Figulla HR. Pentoxifylline in ischemic, hypertensive and idiopathic-dilated cardiomyopathy: effects on left-ventricular function, inflammatory cytokines and symptoms. *Eur J Heart Fail* 6: 195–201, 2004.
2. Baumgarten G, Knuefermann P, Kalra D, Gao F, Taffet GE, Michael L, Blackshear PJ, Carballo E, Sivasubramanian N, Mann DL. Load-dependent and -independent regulation of proinflammatory cytokine and cytokine receptor gene expression in the adult mammalian heart. *Circulation* 105: 2192–2197, 2002.
3. Dujardin KS, Tei C, Yeo TC, Hodge DO, Rossi A, Seward JB. Prognostic value of a Doppler index combining systolic and diastolic performance in idiopathic-dilated cardiomyopathy. *Am J Cardiol* 82: 1071–1076, 1998.
4. Finkel MS, Oddis CV, Jacob TD, Watkins SC, Hattler BG, Simmons RL. Negative inotropic effects of cytokines on the heart mediated by nitric oxide. *Science* 257: 387–389, 1992.
5. Francis J, Beltz T, Johnson AK, Felder RB. Mineralocorticoids act centrally to regulate blood-borne tumor necrosis factor- α in normal rats. *Am J Physiol Regul Integr Comp Physiol* 285: R1402–R1409, 2003.
6. Francis J, Chu Y, Johnson AK, Weiss RM, Felder RB. Acute myocardial infarction induces hypothalamic cytokine synthesis. *Am J Physiol Heart Circ Physiol* 286: H2264–H2271, 2004.
7. Francis J, MohanKumar PS, MohanKumar SM. Lipopolysaccharide stimulates norepinephrine efflux from the rat hypothalamus in vitro: blockade by soluble IL-1 receptor. *Neurosci Lett* 308: 71–74, 2001.
8. Francis J, Wei SG, Weiss RM, Felder RB. Brain angiotensin-converting enzyme activity and autonomic regulation in heart failure. *Am J Physiol Heart Circ Physiol* 287: H2138–H2146, 2004.
9. Francis J, Weiss RM, Wei SG, Johnson AK, Felder RB. Progression of heart failure after myocardial infarction in the rat. *Am J Physiol Regul Integr Comp Physiol* 281: R1734–R1745, 2001.
10. Francis J, Zhang ZH, Weiss RM, Felder RB. Neural regulation of the proinflammatory cytokine response to acute myocardial infarction. *Am J Physiol Heart Circ Physiol* 287: H791–H797, 2004.

11. **Griendling KK, Sorescu D, Ushio-Fukai M.** NAD(P)H oxidase: role in cardiovascular biology and disease. *Circ Res* 86: 494–501, 2000.
12. **Gurantz D, Yndestad A, Halvorsen B, Lunde OV, Omens JH, Ueland T, Aukrust P, Moore CD, Kjekshus J, Greenberg BH.** Etanercept or intravenous immunoglobulin attenuates expression of genes involved in post-myocardial infarction remodeling. *Cardiovasc Res* 67: 106–115, 2005.
13. **Harjai KJ, Scott L, Vivekananthan K, Nunez E, Edupuganti R.** The Tei index: a new prognostic index for patients with symptomatic heart failure. *J Am Soc Echocardiogr* 15: 864–868, 2002.
14. **Heymes C, Bendall JK, Ratajczak P, Cave AC, Samuël JL, Hasenfuss G, Shah AM.** Increased myocardial NADPH oxidase activity in human heart failure. *J Am Coll Cardiol* 41: 2164–2171, 2003.
15. **Irwin MW, Mak S, Mann DL, Qu R, Penninger JM, Yan A, Dawood F, Wen WH, Shou Z, Liu P.** Tissue expression and immunolocalization of tumor necrosis factor- α in postinfarction dysfunctional myocardium. *Circulation* 99: 1492–1498, 1999.
16. **Kang YM, Zhang ZH, Johnson RF, Yu Y, Beltz T, Johnson AK, Weiss RM, Felder RB.** Novel effect of mineralocorticoid receptor antagonism to reduce proinflammatory cytokines and hypothalamic activation in rats with ischemia-induced heart failure. *Circ Res* 99: 758–766, 2006.
17. **Kannan H, Hayashida Y, Yamashita H.** Increase in sympathetic outflow by paraventricular nucleus stimulation in awake rats. *Am J Physiol Regul Integr Comp Physiol* 256: R1325–R1330, 1989.
18. **Kelly RA, Smith TW.** Cytokines and cardiac contractile function. *Circulation* 95: 778–781, 1997.
19. **Krijnen PA, Meischl C, Hack CE, Meijer CJ, Visser CA, Roos D, Niessen HW.** Increased Nox2 expression in human cardiomyocytes after acute myocardial infarction. *J Clin Pathol* 56: 194–199, 2003.
20. **Lindley TE, Doobay MF, Sharma RV, Davisson RL.** Superoxide is involved in the central nervous system activation and sympathoexcitation of myocardial infarction-induced heart failure. *Circ Res* 94: 402–409, 2004.
21. **Mann DL, McMurray JJ, Packer M, Swedberg K, Borner JS, Colucci WS, Djian J, Drexler H, Feldman A, Kober L, Krum H, Liu P, Nieminen M, Tavazzi L, van Veldhuisen DJ, Waldenström A, Warren M, Westheim A, Zannad F, Fleming T.** Targeted anticytokine therapy in patients with chronic heart failure: results of the Randomized Etanercept Worldwide Evaluation (RENEWAL). *Circulation* 109: 1594–1602, 2004.
22. **Meldrum DR, Dinarello CA, Shames BD, Cleveland JC Jr, Cain BS, Banerjee A, Meng X, Harken AH.** Ischemic preconditioning decreases postischemic myocardial tumor necrosis factor- α production Potential ultimate effector mechanism of preconditioning. *Circulation* 98: II214–II219, 1998.
23. **Moe KT, Aulia S, Jiang F, Chua YL, Koh TH, Wong MC, Dusting GJ.** Differential upregulation of Nox homologues of NADPH oxidase by tumor necrosis factor- α in human aortic smooth muscle and embryonic kidney cells. *J Cell Mol Med* 10: 231–239, 2006.
24. **Moller JE, Sondergaard E, Poulsen SH, Egstrup K.** The Doppler echocardiographic myocardial performance index predicts left-ventricular dilation and cardiac death after myocardial infarction. *Cardiology* 95: 105–111, 2001.
25. **Myers SI, Horton JW, Hernandez R, Walker PB, Vaughan WG.** Pentoxifylline protects splanchnic prostacyclin synthesis during mesenteric ischemia/reperfusion. *Prostaglandins* 47: 137–150, 1994.
26. **Patel KP.** Role of paraventricular nucleus in mediating sympathetic outflow in heart failure. *Heart Fail Rev* 5: 73–86, 2000.
27. **Pyner S, Coote JH.** Identification of branching paraventricular neurons of the hypothalamus that project to the rostroventrolateral medulla and spinal cord. *Neuroscience* 100: 549–556, 2000.
28. **Schermuly RT, Roehl A, Weissmann N, Ghofrani HA, Leuchte H, Grimminger F, Seeger W, Walmrath D.** Combination of nonspecific PDE inhibitors with inhaled prostacyclin in experimental pulmonary hypertension. *Am J Physiol Lung Cell Mol Physiol* 281: L1361–L1368, 2001.
29. **Skudicky D, Bergemann A, Sliwa K, Candy G, Sareli P.** Beneficial effects of pentoxifylline in patients with idiopathic dilated cardiomyopathy treated with angiotensin-converting enzyme inhibitors and carvedilol: results of a randomized study. *Circulation* 103: 1083–1088, 2001.
30. **Sliwa K, Skudicky D, Candy G, Bergemann A, Hopley M, Sareli P.** The addition of pentoxifylline to conventional therapy improves outcome in patients with peripartum cardiomyopathy. *Eur J Heart Fail* 4: 305–309, 2002.
31. **Sliwa K, Skudicky D, Candy G, Wisenbaugh T, Sareli P.** Randomised investigation of effects of pentoxifylline on left-ventricular performance in idiopathic dilated cardiomyopathy. *Lancet* 351: 1091–1093, 1998.
32. **Sliwa K, Woodiwiss A, Candy G, Badenhorst D, Libhaber C, Norton G, Skudicky D, Sareli P.** Effects of pentoxifylline on cytokine profiles and left ventricular performance in patients with decompensated congestive heart failure secondary to idiopathic dilated cardiomyopathy. *Am J Cardiol* 90: 1118–1122, 2002.
33. **Sliwa K, Woodiwiss A, Kone VN, Candy G, Badenhorst D, Norton G, Zambakides C, Peters F, Essop R.** Therapy of ischemic cardiomyopathy with the immunomodulating agent pentoxifylline: results of a randomized study. *Circulation* 109: 750–755, 2004.
34. **Strieter RM, Remick DG, Ward PA, Spengler RN, Lynch JP, 3rd Larrick J, Kunkel SL.** Cellular and molecular regulation of tumor necrosis factor- α production by pentoxifylline. *Biochem Biophys Res Commun* 155: 1230–1236, 1988.
35. **Swanson LW, Sawchenko PE.** Hypothalamic integration: organization of the paraventricular and supraoptic nuclei. *Annu Rev Neurosci* 6: 269–324, 1983.
36. **Tei C, Ling LH, Hodge DO, Bailey KR, Oh JK, Rodeheffer RJ, Tajik AJ, Seward JB.** New index of combined systolic and diastolic myocardial performance: a simple and reproducible measure of cardiac function—a study in normals and dilated cardiomyopathy. *J Cardiol* 26: 357–366, 1995.
37. **Torre-Amione G, Kapadia S, Lee J, Durand JB, Bies RD, Young JB, Mann DL.** Tumor necrosis factor- α and tumor necrosis factor receptors in the failing human heart. *Circulation* 93: 704–711, 1996.
38. **Ungvari Z, Csizsar A, Edwards JG, Kaminski PM, Wolin MS, Kaley G, Koller A.** Increased superoxide production in coronary arteries in hyperhomocysteinemia: role of tumor necrosis factor- α , NAD(P)H oxidase, and inducible nitric oxide synthase. *Arterioscler Thromb Vasc Biol* 23: 418–424, 2003.
39. **Zhang M, Xu YJ, Saini HK, Turan B, Liu PP, Dhalla NS.** Pentoxifylline attenuates cardiac dysfunction and reduces TNF- α level in ischemic-reperfused heart. *Am J Physiol Heart Circ Physiol* 289: H832–H839, 2005.
40. **Zhang Y, Yu Y, Zhang F, Zhong MK, Shi Z, Gao XY, Wang W, Zhu GQ.** NAD(P)H oxidase in paraventricular nucleus contributes to the effect of angiotensin II on cardiac sympathetic afferent reflex. *Brain Res* 1082: 132–141, 2006.
41. **Zhang ZH, Wei SG, Francis J, Felder RB.** Cardiovascular and renal sympathetic activation by blood-borne TNF- α in rat: the role of central prostaglandins. *Am J Physiol Regul Integr Comp Physiol* 284: R916–R927, 2003.